



AIAA 99-3786

**Molecular Tagging Velocimetry (MTV):
Progress and Applications (Invited)**

M. M. Koochesfahani
Department of Mechanical Engineering
Michigan State University
East Lansing, Michigan

30th AIAA Fluid Dynamics Conference
28 June - 1 July, 1999 / Norfolk, VA

Molecular Tagging Velocimetry (MTV): Progress and Applications

Manoochehr Koochesfahani*
Department of Mechanical Engineering
Michigan State University, East Lansing, Michigan

This paper describes some of the recent progress in Molecular Tagging Velocimetry and its applications. A brief overview of the different molecular tagging methods mostly in use today is given. Improvements in tagging, detection, and processing schemes, allow whole-field measurements of two components of the velocity vector simultaneously at more than 600 points over a plane with sufficient accuracy to make this technique a viable tool for fluid flow studies. Application of MTV to several flow fields are described to highlight some of the capabilities of this technique. The examples include boundary-layer resolved measurements of unsteady boundary layer separation, slow convective flow in directional solidification, intake flow into a model IC engine, and the hot flow in late compression of a motored IC engine. Finally, examples are given to illustrate the potential for simultaneous flow visualization/passive scalar and velocity measurements, as well as three-component velocimetry using stereo imaging.

1. Introduction

Use of molecular tagging approaches for fluid flow velocimetry is a relatively recent development. A variety of molecules have been utilized for this purpose and, regardless of the details of the photophysics of each, their application to fluid dynamics measurements can be discussed under a common heading of Molecular Tagging Velocimetry (MTV). This method of velocimetry relies on molecules that can be turned into long lifetime tracers upon excitation by photons of an appropriate wavelength. Typically a pulsed laser is used to “tag” the regions of interest, and those tagged regions are interrogated at two successive times within the lifetime of the tracer. The measured Lagrangian displacement vector provides the estimate of the velocity vector. This technique can be thought of as essentially the *molecular* counterpart of Particle Image Velocimetry (PIV), and complements it where the use of seed particles is either not desirable or may lead to complications connected to tracking the flow, density mismatch, particle seeding density or strong out-of-plane motions.

A new user of the MTV approach is confronted with basically two primary issues: the choice of the molecular tracer, and the actual implementation in terms of the method of tagging, detection, and data processing. There is often no standard method of implementing MTV and each user has to adapt the technique to the unique aspects and specific demands of the particular flow under investigation. For example, the tracer is first

selected based on the fluid medium and the range of speeds to be measured in a flow, in conjunction with flow facility compatibility issues. Sometimes a suitable tracer may not exist at all. The photophysics of the tracer, in turn, dictates the type and number of photon sources needed. The method of tagging and detection are determined by how many velocity components need to be measured and the required accuracy of those measurements. The sensitivity and signal to noise characteristics of detection play a major role in the accuracy of the displacement measurements and also impacts the minimum required laser energy. The tagging method can influence the choice of the data processing scheme for extracting the displacement information.

Considering the number of inter-related issues involved, the best way to succeed is perhaps to become familiar with the advantages and disadvantages of all the different available methods for each step. One can then “pick and choose” from a “toolbox” of these different methods the combinations that better suite the particular application. Having this approach in mind, the purpose of this paper is to give a brief overview of the different molecular tagging methods mostly in use today including the developments from our group. Examples of our application of MTV to various flow fields are provided to highlight some of the capabilities of this technique. These examples include boundary-layer resolved measurements of unsteady boundary layer separation, slow convective flow in directional solidification, intake flow into a steady model of an IC engine, and the hot flow in late compression of a motored IC engine. The capability of MTV for velocimetry in highly 3-D flows with strong out-of-plane motions has been demonstrated also, but will not be described here. Finally examples are given to illustrate the potential for simultaneous flow visualization/passive scalar and velocity measurements,

Copyright © 1999 by M. Koochesfahani. Published by the American Institute of Aeronautics and Astronautics, Inc. with permission.

* Associate Professor

and three-component velocimetry using stereo imaging.

2. Molecular Tracers

A molecular complex is suitable for molecular tagging applications if its lifetime as a tracer is long enough relative to the flow convection time scale to allow sufficient displacement of the tagged regions. It is also important to recognize that, in practice, the maximum needed lifetime of a tracer for a given flow field is dictated by the sensitivity of detection; see example 2 in Section 3. In this section the primary molecular tracers in use today for liquid and gas phase applications are described. The reader is encouraged to consult the cited references for each case for further details. Two earlier reviews^{1,2} also contain information on this topic.

2.1 Liquid-Phase Applications

Three molecular tracers have been most widely used to date: photochromic molecules, caged fluorescent compounds, and specially engineered water-soluble phosphorescent supramolecules. Since none of them is naturally present in the flowing media where they are typically used, these molecules are first premixed in the flowing liquid. All the liquid-phase flow examples given in Section 4 of this paper take advantage of phosphorescent supramolecules.

MTV investigations in liquid-phase flows have, until recently, relied on photochromic molecules. In a photochromic process a molecule M is excited to produce a high energy form of M , designated M' , which has a different absorption spectrum giving rise to a color change (e.g. from clear to dark blue). The long lifetime tracer is the newly produced M' , which persists for several seconds to minutes. The tagging process (i.e. the nonradiative conversion from M to M') occurs rapidly (within the duration of a few nanosecond long laser pulse). The photochromic process is reversible, therefore the chemical is reusable. Photochromic dyes are generally insoluble in water, so organic liquids such as kerosene are typically used as the flowing medium. The use of photochromic chemicals requires two photon sources; typically a UV laser (e.g. $\lambda = 351$ nm) to induce the color change and a white light source to interrogate the tagged regions convected by the flow. Hummel and his group^{3,4} originated the use of photochromic chemicals as a velocity measurement tool using tagging along single lines. Significant improvements were made in the work of Falco & Chu⁵, who used grid illumination to tag the molecules and coined the acronym LIPA (Laser Induced Photochemical Anemometry). Some of the advantages of photochromics (long lifetime, reusable)

are offset by the need to use special fluids such as kerosene. It is possible to ease this restriction by making chemical modifications to enable many photochromic dyes to dissolve in water^{6,7}. The most significant drawback in using photochromic chemicals is that the image is produced by a change in absorbance, thereby requiring a measurement of the difference between incident and transmitted light. Emitted light (against a black background) is more easily and accurately detected than transmitted light; consequently, images based on luminescence are better suited to MTV applications. Nevertheless, photochromics are being used effectively to advance the understanding of flow physics⁸⁻¹⁰.

Caged fluorescein and similar water-soluble compounds have recently become available, and their use was first introduced by Lempert, et al.¹¹ under the acronym PHANTOMM (PHoto-Activated Non-intrusive Tracking of Molecular Motion). In this compound a chemical group is attached to fluorescein in order to render it non-fluorescent. The caging group is removed upon absorption of UV photons ($\lambda = 350$ nm), thereby creating regular fluorescein which fluoresces with a very high quantum efficiency. Here the long-lifetime tracer is the uncaged fluorescein, which persists for a very long time and can be interrogated at the time of interest through its luminescence upon re-irradiation. Two sources of photons are therefore needed, one to break the cage and the other to excite fluorescence. Two aspects of the current design of caged fluorescein require special attention when designing an experiment: The cage-breaking process is irreversible, so each caged molecule can be used only once. The cage-breaking process is not rapid and occurs with a time constant on the order of a few milliseconds. The delay between laser tagging and the generation of enough fluorescein to obtain an image with sufficient signal/noise dictates the fastest flow speeds that can be accommodated. On the other hand, very slow speed flows can be handled with ease considering the very long lifetime (practically infinite) of the uncaged fluorescein. Several novel applications using caged fluorescein have already been reported¹²⁻¹⁴.

Phosphorescent supramolecules are a new class of water-soluble compounds suitable for molecular tagging diagnostics. When a phosphorescent compound is used for molecular tagging, excitation by photons produces a long-lived excited state which is interrogated through its phosphorescence emission as the molecule radiatively returns to its ground state. The long lifetime tracer is the excited state molecule itself. In this case only one source of photons is needed, the tagging process occurs during the laser pulse (a few nanoseconds in our case), and the excitation/emission process is reversible, which means the chemicals are reusable. The difficulty is that long-

lived excited states (i.e. phosphorescence) suffer from O_2 and H_2O quenching, and as a result, suitable molecular complexes have not been available until recently. New findings by Nocera and his group¹⁵⁻¹⁷ have shown that supramolecules may be designed to exhibit long-lived phosphorescence which is not quenched. The design prevents the quenching of a lumophore by mixing certain alcohols (indicated collectively by “ROH”) with an aqueous solution of a cyclodextrin (CD) cup that contains the lumophore. Cyclodextrins are molecules constructed from sugars connected in a head-to-tail arrangement forming a cup-shaped cavity. The CD used in the applications to date is GB-CD, which is constructed of 7 glucose subunits with one additional glucose bonded to the rim of the cup to improve its solubility in water, the lumophore is 1-bromonaphthalene (1-BrNp) which absorbs efficiently at $\lambda = 308$ nm, and the alcohol is typically cyclohexanol. According to previous studies^{15,16} the addition of alcohol forms a ternary complex (1-BrNp · G β -CD · ROH), where the alcohol hydrogen bonds to the rim of the CD cup and acts as its lid, thereby shielding 1-BrNp from oxygen. (For this particular supramolecule the phosphorescence is not significantly quenched by H_2O .) The resulting long-lived, green phosphorescence has a typical lifetime $\tau = 5$ ms. Further details of the properties of these compounds relevant to the optical design of an MTV implementation are found in Gendrich, et al.¹⁸.

One disadvantage of the phosphorescent supramolecules described here is their lower quantum efficiency ($\phi_e = 0.035$) compared to that of uncaged fluorescein ($\phi_e = 0.90$). This is offset, however, by the advantages of reusability, the need for only one photon source, and a lower cost (estimated to be between 5 to 100 times less, depending on whether a CW or pulsed laser source is used to interrogate the uncaged fluorescein). Regardless of these comparisons, very low speed flows necessitating extremely long delay times between tagging and interrogation are best investigated using caged fluorescein or photochromic dyes. In this connection, it is again useful to recall that luminescence lifetime refers to the time when the emission has decayed to 37% (e^{-1}) of its initial intensity. When using a phosphorescent complex, the actual usable delay time between laser tagging and interrogation can be considerably longer than the lifetime and is dictated by the sensitivity of detection used; see example in Section 4.2. Utilization of phosphorescent compounds has been reported in a variety of recent fluid flow studies^{2, 18-24}.

2.2 Gas-Phase Applications

The majority of gas-phase applications to date have

taken advantage of excited-state oxygen, ozone (O_3), OH, and phosphorescent molecules such as biacetyl. The first three molecular tracers are generated from species naturally present in air, i.e. oxygen and water vapor in humid air or that generated as a result of combustion. As a result, their use is often referred to as “unseeded” application. By contrast, biacetyl must first be seeded into the flowing gas stream. All the gas-phase flow examples given in Section 4 of this paper take advantage of biacetyl’s phosphorescence.

The use of excited-state oxygen fluorescence was pioneered by Miles, et al.²⁵⁻²⁸ under the acronym RELIEF (Raman Excitation + Laser-Induced Electronic Fluorescence of oxygen). In this approach, stimulated Raman scattering is used to drive oxygen into the vibrationally excited state through a nonlinear process requiring simultaneous two-photon excitation. The long lifetime molecular tracer is the vibrationally excited O_2 which forms rapidly (within the order of 10 ns long duration of a laser pulse). The location of the tagged region displaced by the flow is determined by interrogating the vibrationally excited O_2 through its fluorescence when excited by an ArF excimer laser ($\lambda = 193$ nm). The use of RELIEF approach, therefore, requires three sources of photons, two for tagging and one for interrogation. The lifetime of the vibrationally excited O_2 tracer depends on the presence of quenchers in the flow, e.g. water vapor. The majority of RELIEF applications have been in high-speed flows with the time delay between tagging and interrogation of order 10 μ s or less, although time delays of order 100 μ s should be possible in pure oxygen or air. It is worth noting that tagging by a nonlinear optical process requires high intensity sources, and it may be difficult to tag large regions (i.e. dimensions larger than of order 1 cm) in a flow.

In a more recent unseeded method of velocimetry, the use of ozone (O_3) has been developed by Pitz, et al.²⁹⁻³¹ under the acronym OTV (Ozone Tagging Velocimetry). In this method, the long lifetime tracer is O_3 which is generated by photodissociation of O_2 using a pulsed ArF excimer laser ($\lambda = 193$ nm). The tagged regions are interrogated by a KrF excimer laser ($\lambda = 248$ nm) through O_3 dissociation followed by O_2 fluorescence. Two sources of photons are therefore needed for this approach. The ozone tracer is a very long-lived molecular tracer in dry or humid air at room temperature, and even in the presence of NO. The delay times between tagging and interrogation of order milliseconds have been reported, making OTV suitable for low speed flows as well. When applying this technique to high speed flows, one should be aware of the fact that the formation of this molecular tracer (i.e. O_3 production) is not rapid and occurs over a time scale

of 20 μs (time to reach 50% of maximum concentration). In a situation similar to caged fluorescein, the delay between laser tagging and the generation of enough ozone to obtain an image with sufficient signal/noise dictates the fastest flow speeds that can be accommodated. Ozone tagging is not practical for hot flows (e.g. temperature beyond 500 K) due to the thermal decomposition of O_3 soon after formation.

In yet another unseeded method of velocimetry for flows which contain water vapor, photon excitation is used to generate OH by photodissociation of H_2O . The long lifetime tracer is OH which is then interrogated through its fluorescence using a second photon source. The original development of this tagging approach^{32,33} utilized two-photon photodissociation of water vapor using a 248 nm excimer laser and the resulting OH was interrogated by its fluorescence excited at 308 nm. Advances in this approach have recently been reported^{34,35} under the acronym HTV (Hydroxyl Tagging Velocimetry). In these developments, single-photon dissociation of vibrationally-excited water vapor by an ArF excimer laser ($\lambda = 193$ nm) generates OH photoproducts at a concentration higher than the ambient. The tagged regions are interrogated using OH fluorescence caused by excitation from a KrF excimer laser ($\lambda = 248$ nm). The utility of OH tagging is primarily to high temperature, high speed flow fields³⁵. The recent developments under HTV have increased the size of the region that can be tagged due to the single-photon process used. In addition, since HTV and OTV use common photon wavelengths for tagging and interrogation, both can be used simultaneously to quantify the velocity field in adjacent low and high temperature flows typical of combustion environments.

Some of the popular tracers such as biacetyl and acetone, which have often been used for flow visualization and LIF concentration measurements, also exhibit phosphorescence which can be used for MTV applications. In this case only one photon source is needed. The tagging process occurs during the brief laser pulse and the long lifetime tracer is the excited state molecule itself. However, because phosphorescence of these molecules is effectively quenched by oxygen, their use is limited to oxygen-free environments (typically N_2 is used). Even though the potential of biacetyl as a molecular tracer for velocimetry has been known for sometime³⁶⁻³⁹, it is only recently that detailed multi-point measurements have been carried out with it⁴⁰⁻⁴². The properties of biacetyl (also called 2,3-Butanedione) have been studied extensively in the past. It is non-toxic (actually a food additive with a butter smell), and its relatively high vapor pressure (40 Torr at room temperature) allows a molar seeding fraction of about 5%. Biacetyl has a broad absorption spectrum with two

peaks at 270 nm, and 420 nm⁴². In our work (see Section 4), a XeCl excimer laser ($\lambda = 308$ nm) is usually used as the excitation source. The long-lived phosphorescence of biacetyl can have a lifetime as high as 1.5 ms in the absence of oxygen. The observed lifetime can be lower in practice due to increasing photon flux and small amounts of oxygen in the flow system; a lifetime of order 100 μs is typical in our experiments. Some of the advantages of using biacetyl are that only one photon source is needed and UV detection is not necessary (phosphorescence emission is green/yellow). However, because its use is limited to oxygen-free flows, biacetyl is not a practical molecular tag for general wind tunnel use.

3. Details of MTV Implementation

Regardless of the different complexities of the photophysics of the molecular tracers used for MTV, they all share certain common issues when they are applied to study fluid flows. These issues are discussed in this section. The details of implementation play an important role in making such techniques accurate and useful tools for flow studies.

3.1 Tagging Methods

Tagging along single or multiple lines is perhaps the simplest method of tagging and has been utilized in a large fraction of studies to date^{3,4,11-14,21,25-29,36}. The velocity is determined from the displacement of the tagged lines in much the same manner as using hydrogen bubble lines generated by a wire⁴³. An example of line tagging is shown in Figure 1 illustrating the region (about 28 mm \times 24 mm) downstream of a nitrogen round jet (diameter 7 \approx mm) seeded with biacetyl. The jet speed is approximately 180 m/s and the image is captured 10 μs after laser firing. The first tagged line visible on the left is located about 1.2 jet diameters downstream of the nozzle lip. The displacement of the tagged lines clearly shows the general evolution in the jet potential core. The maximum displacement of the tagged line in the center of the jet is about 1.8 mm (nearly 18 pixels).

It is very important to recognize that line tagging allows the measurement of only one component of velocity, that normal to the tagged line. In addition, the estimate of this velocity component has an inherent error associated with it, which is connected with the ambiguity in the unique determination of the displacements of various portions of a (continuous) tagged line. Following previous analyses^{2,21}, this error can be cast in the form $\Delta u/u = \tan\theta (\partial u/\partial y) \Delta t$, where u is the estimated velocity component normal to the tagged line, Δu is the error in the estimated velocity, θ is the local flow angle given by

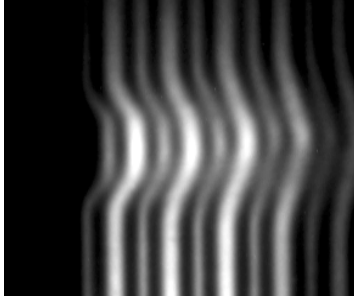


Fig. 1. Multiple line tagging downstream of a N_2 jet seeded with biacetyl. Flow is from left to right.

$\tan \theta = v/u$ with v being the flow velocity parallel to the tagged line, and Δt is the time delay between tagging and interrogation. Clearly an *a priori* knowledge of the flow field is necessary in order to provide an estimate of the error. It can be observed, however, that this inherent error is identically zero only in flows where the velocity component v along the tagged line is zero (i.e. unidirectional flows) or where the velocity gradient along the line $\partial u/\partial y = 0$. In a general flow field where these constraints are not met, the error can be reduced by decreasing the delay time Δt , but it cannot be made arbitrarily small, since Δt has to be large enough for the resulting displacement of the tagged line to be measured with adequate accuracy. While keeping these issues in mind, it is sometimes possible to take advantage of an *a priori* knowledge of the flow field under investigation to design the experimental parameters such that the inherent error discussed here becomes minimal compared to other measurement errors²¹.

In order to unambiguously measure two components of the velocity in a plane, the luminescence intensity field from a tagged region must have spatial gradients in two, preferably orthogonal, directions. For single-point velocimetry, this is easily achieved using a pair of crossing laser beams; a grid of intersecting laser lines allows multi-point velocity measurements. This tagging scheme, first suggested by D'Arco, et al.⁴⁴ and later improved upon and utilized by Falco & Chu⁵, is commonly used these days. In our method of implementation, described in details elsewhere¹⁸, the main beam of an excimer laser is manipulated by cylindrical optics to increase its aspect ratio. The outgoing beam is split using a 50:50 beam splitter, and then each of the resultant beams passes through a beam blocker to generate the laser grid pattern. Spherical lenses are used as needed to control the spatial scaling of the entire grid pattern. The beam blocker is simply a metallic plate with a series of thin slots to block a portion of the incident beam. Even though the beam blockers allow a smaller fraction of the total laser energy

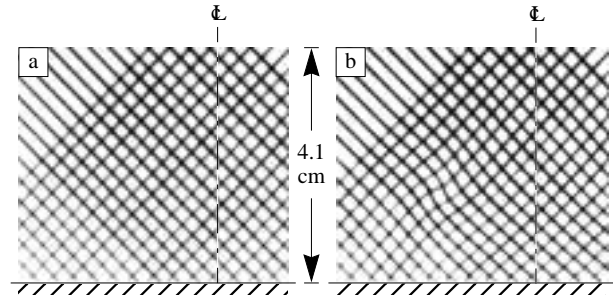


Fig. 2. Tagging by a grid and the resulting MTV image pair: (a) $1 \mu s$ after laser pulse; (b) 8 ms later. Dashed lines indicate the vortex ring axis of symmetry.

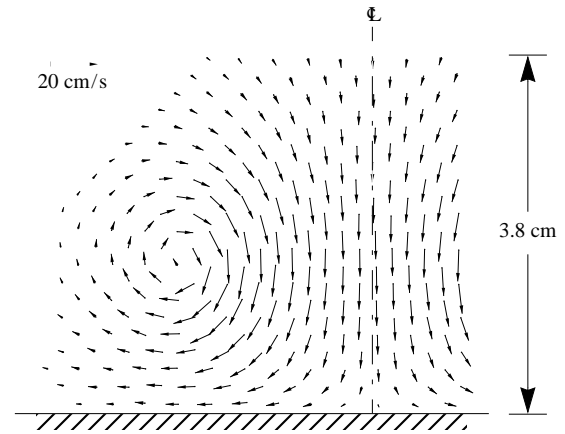


Fig. 3. The velocity field derived from the image pair in Fig. 2 using a spatial correlation approach.

to be used for tagging purposes, they offer a simple way to generate arbitrary slot patterns for optimizing the width and the number of laser lines for a particular experiment, or when beams of non-uniform thickness are needed to simplify the spatial correlation procedure (described in Section 3.3). Figure 2 shows an example of a region tagged by a grid pattern generated in this manner using a beam blocker with nearly uniform slot width and spacing. This example, taken from a water study of the flow field of a vortex ring impacting a solid wall at normal incidence^{18,22}, shows both the initially tagged regions and their subsequent evolution after a time delay. The resultant velocity vector field derived from this image pair (see Section 3.3) is depicted in Figure 3.

Tagging by a non-uniform laser illumination in the form of a grid is needed when the molecular tracer is present uniformly in the fluid. This method is only a special case of a more generalized approach to induce a spatially non-uniform luminescence intensity in a tagged region. For example, the non-uniform passive scalar field typical of most turbulent flows can sometimes be used as a natural source of luminescence non-uniformity

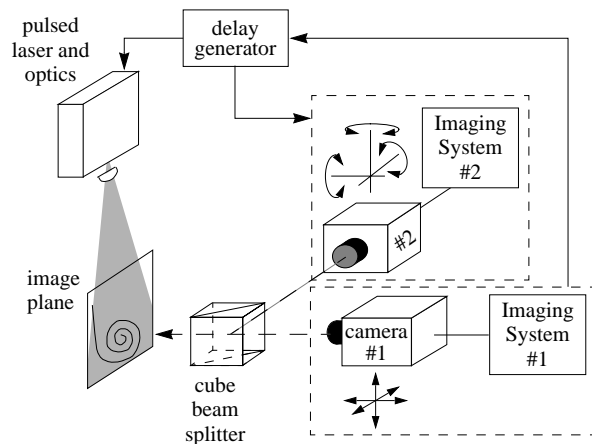


Fig. 4. Optical and electronic arrangement for 2-camera MTV experiments. Both cameras view the same image plane through the cube beam splitter. Synchronization between the two cameras and laser is provided by a digital delay generator.

without the need for grid illumination, or further enhancement of the effect of grid illumination. Examples of this type have been given previously^{2,18}.

In our work involving both liquid phase and gas phase flows, 25×25 grid patterns resulting in the simultaneous measurement of over 600 independent velocity vectors per plane are common. In a recent work²⁴ between 600 to 800 vectors were measured per plane. The limitation in our work is not the available laser energy; the energy for each tagging beam is in the range 1-2 mJ or less for the gas-phase and liquid-phase flows we have studied. Instead, the maximum vector density per plane is limited by the pixel density of our current detector arrays which are nominally in the 512×512 pixel range. It is expected that the velocity measurement density will increase proportionally as denser detector arrays are utilized.

3.2 Detection

The common element among most previous studies is that a single detector is used; the initial (or reference) tagging pattern is recorded once, usually at the beginning of the experiment, and then the “delayed” images are acquired. This approach works well as long as the initial tagging pattern remains spatially invariant throughout the experiment. Otherwise, any variations in the initial pattern (e.g. due to laser beam pointing instability, vibration of the optics, non-uniform tracer distribution, etc.) could be misinterpreted as flow velocity fluctuations. In order to minimize the potential problem just noted, and to create a more flexible system to accommodate cases where no assumption can be made *a priori* about the intensity field in a tagged region, we

have implemented a two-detector imaging system^{2,18}. The experimental arrangement, shown in Figure 4, involves a link between the pulsed laser and the two image detectors through a digital delay generator. Immediately after the laser fires, the first detector records an initial image of the tagged flow, and after a prescribed time delay Δt , the second detector records a later image. In our work utilizing phosphorescent tracers, only a single laser is involved. For tracers requiring a second photon source for interrogation through fluorescence, the second laser would be required to output two pulses Δt apart.

In the arrangement shown in Figure 4, the two detectors view the same region of interest in the flow through a cube beam splitter. The two cameras are typically aligned to better than a pixel; the relative displacement field between the two detectors is taken into account when computing the actual displacement due to the flow for each image pair. The selection of the time delay between tagging and interrogation is dictated by several factors. A larger delay will produce larger displacements and therefore a higher dynamic range in the velocity measurement. However, an increase in Δt often leads to a degraded S/N in the delayed image, which reduces the sub-pixel accuracy in determining the displacement (see next section). For the typical values of Δt in our experiments, we obtain maximum displacements in the range of 10 pixels corresponding to a real displacement in the range of 0.4 to 1.5 mm, depending on the image ratio.

It is clear that single camera detection will be adequate as long as the initial tagging pattern varies less than the sub-pixel accuracy required of the displacement measurement. Depending on the image field of view, a typical 0.1 sub-pixel accuracy (see Section 3.3) would suggest that the initial tagging pattern would have to be invariant to within a few microns. As new detector technologies develop, the possibility of replacing the two-detector system with “double-frame” single cameras, or other such variations, certainly exists¹⁸. Most gas-phase applications have utilized gated image-intensified detectors, whereas for some liquid-phase applications standard CCD cameras are adequate. In our work in liquid-phase, we use non-intensified frame transfer cameras typically for fields of view larger than about 3 cm. For smaller fields of view, and in gas-phase applications, we use gated image-intensified detectors. These detectors are all nominally 512×512 pixel arrays operating at 30 frame/s. The images are digitized to 8 bits by two image acquisition/ processing systems and transferred onto high capacity disk arrays in real time.

3.3. Processing

It is desirable to determine the displacement vector of the tagged regions with the highest possible sub-pixel accuracy in order to increase the dynamic range of the velocity measurements. In addition, for a given required dynamic range, a higher sub-pixel accuracy will allow a shorter time delay Δt to be used between the two images, thereby increasing the bandwidth in measuring unsteady flow phenomena.

The usual method for finding the displacement of tagged lines or grids has been to locate the center of each line through various techniques. Most of the recent techniques use the best fit to an assumed laser line shape, for example, a gaussian intensity distribution. A systematic statistical study of the performance of this approach while considering the effects of experimental parameters such as image signal to noise ratio has not been reported. However, a recent study²¹ gives the accuracy in determining the displacement vector to be ± 0.35 pixel rms. The performance of this method will suffer when the intensity distribution of the tagged regions cannot be assumed in advance, for example, due to non-uniform tracer distribution, difficulties associated with laser beam transmission through a flowing medium, bleaching effects, etc.

We have taken a different approach in an attempt to implement a generalized scheme that is independent of the specific intensity distribution within a tagged region and which can accommodate arbitrary tagging patterns including those due to non-uniform scalar mixing fields. The displacement of the tagged regions is determined using a direct digital spatial correlation technique. The details of this approach and its performance are described elsewhere⁴⁵. A small window, referred to as the source window, is selected from a tagged region in the earlier image, and it is spatially correlated with a larger roam window in the second image. A well-defined correlation peak occurs at the location corresponding to the displacement of the tagged region by the flow; the displacement peak is located to sub-pixel accuracy using a multi-dimensional polynomial fit. This procedure is similar to what could be used in DPIV processing of particle image pairs. One advantage of this processing technique over traditional line-center methods is robustness to the presence of noise due to the averaging process inherent in the correlation procedure. Based on both experiments and an extensive statistical study on the performance of this correlation approach, we have found that we can typically measure the displacement of the tagged regions with a 95% confidence limit of ± 0.1 sub-pixel accuracy (i.e. 95% of the displacement measurements are accurate to better than 0.1 pixel). This corresponds to an rms accuracy of ± 0.05 pixel, assuming

a Gaussian distribution for error. For high values of image S/N, the 95% confidence level can be as high as 0.015 pixel⁴⁵.

An example of the application of this processing method was shown in Figure 3 (data shown are "raw" and not post-processed), and several more will be described in the next section. The processing of long sequences of MTV image pairs has been automated through a common C algorithm running on both Unix and PC systems. While running on a Silicon Graphics R-10000 CPU, the processing speed is about 40 vector/s and about 50% slower when running on a 400-MHZ PentiumII PC. The algorithm has not been optimized for processing speed and improvements are likely.

4. Examples of MTV Measurements

This section describes several examples to illustrate some of the capabilities of the MTV technique for studying fluid flows. Measurements have also been carried out successfully in flows with strong out-of-plane motions where the primary flow direction is normal to the tagged plane^{2,24}, but those will not be discussed here. In all the measurements described here a Lambda Physik XeCl excimer laser ($\lambda = 308$ nm) was used to provide 20 ns pulses with a pulse energy between 50 and 200 mJ. As mentioned earlier, the energy per tagging beam is in the range 1-2 mJ or less. The detectors utilized are Pulnix (TM-9701) frame transfer (non-intensified) CCD cameras and Xybion (ISG-350-GW3) gated image-intensified cameras, all operating at 30 frame/s.

4.1 Boundary-Layer Resolved Measurements of Pitching Airfoil Leading-Edge Separation

When an airfoil dynamically pitches to high angles of attack the viscous boundary layer near the leading edge eventually separates and causes catastrophic events such as dynamic stall. Two-dimensional Navier-Stokes computations have been available for this flow field in the Reynolds number range $Re_c = 10^4$, where the boundary layer is laminar and the computations can avoid the artifacts of turbulence modeling. However, the details of the flow within the boundary layer at the onset of separation have not been captured experimentally to date. MTV measurements have recently been completed²³, providing the first detailed map of the events that occur within the boundary layer near the surface of a pitching airfoil. This is an example of the type of detailed measurements that are possible with molecular tagging techniques in studying fundamental flow phenomena.

The measurements are carried out in a 60 cm \times 60 cm water tunnel using a 12-cm chord NACA-0012 airfoil

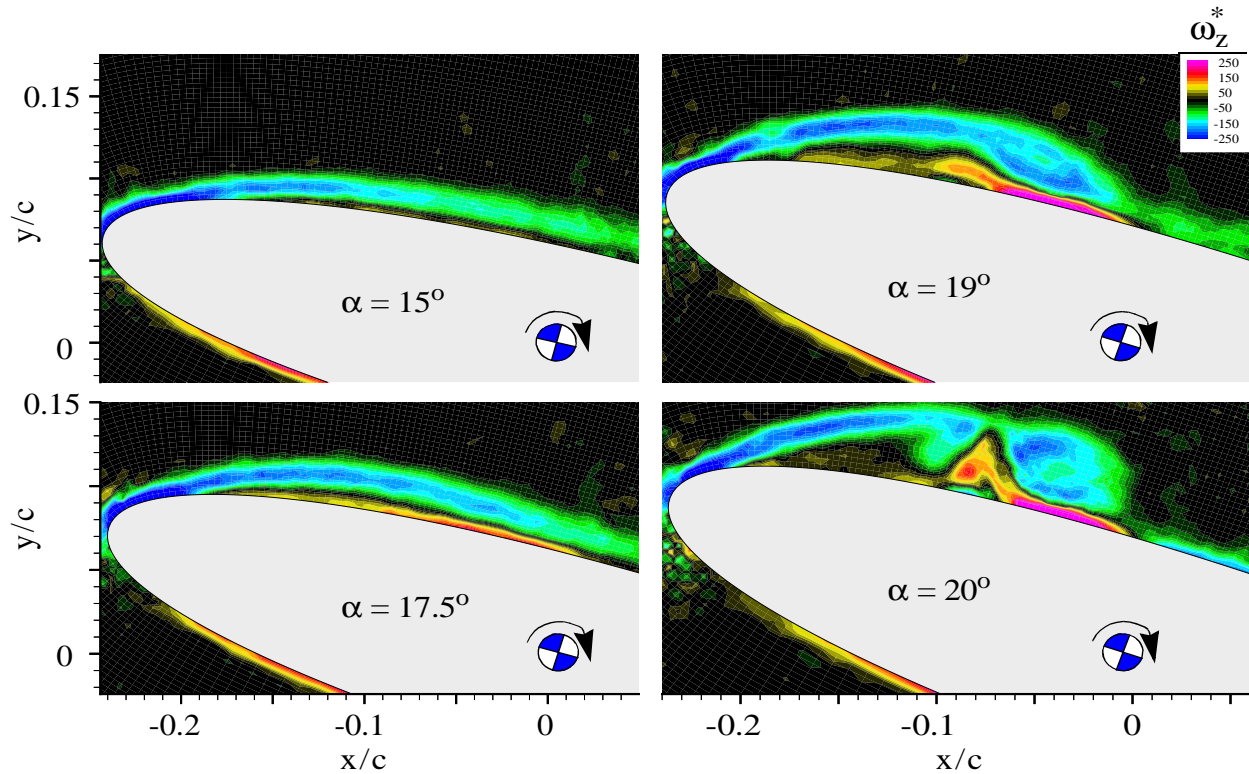


Fig. 5. Evolution of vorticity field and onset of leading-edge separation on an airfoil pitching to high angles of attack.

pitching at a constant rate (non-dimensional pitch rate = 0.1) from 0 to 60 degrees angle of attack. The chord Reynolds number is about 12,000. The parameters of the experiment are selected to match the complementary computations performed earlier. The range of spatial scales in this problem is larger than those we are able to resolve with a single field of view, bearing in mind the maximum vector density we can measure currently (see Section 3.1). As a result, these measurements are carried out over multiple fields of view with decreasing size producing a large data set (117 GB of image data). The success of this approach requires sufficient repeatability of the flow features, a requirement that is satisfied for the cases shown here. The data from different fields of view are compiled into a single data set with over 10,000 velocity vectors per plane for each 0.25 degree change in angle of attack. The non-dimensional vorticity field computed from this data set at four angles of attack near the onset of leading-edge separation is shown in Figure 5. Among the details resolved in these measurements are the occurrence of a thin reversed flow region near the airfoil surface, and the eruption of the boundary layer vorticity away from the wall in a highly localized manner (both in time and space). A conclusion from our experimental data is that the process of boundary layer separation occurs over a shorter time scale, and is more eruptive, than that captured by the computations.

4.2 Measurement of Buoyancy-Driven Convective Flow during Solidification

Solidifying a binary alloy under off-eutectic conditions is often accompanied by convection in the melt. The convection mechanisms caused by solutal and thermal forces for such conditions can produce inhomogeneities and imperfections such as solute-rich channels in the final fully solidified ingot casting. While the convective phenomena involved in the formation of these imperfections are not completely understood, it is generally accepted that they are best described in terms of complex dynamic fields and that most experimental methods applied to date are poorly suited to measure these fields. One means of learning more about these phenomena has been the use of transparent analogs of metallic alloys. One such analog is the binary aqueous ammonium chloride ($\text{NH}_4\text{Cl}-\text{H}_2\text{O}$) system. Some of the complex features of convective phenomena associated with solidification in the aqueous ammonium chloride include: the vertical growth of a solid/liquid interface with concurrent early development of numerous fine structures of salt fingers followed by the appearance of a small number of plumes ejecting fluid jets from channels in the mushy zone of the growing dendritic crystal mass. The shadowgraph picture in Figure 6 illustrates a small number of relatively large plumes

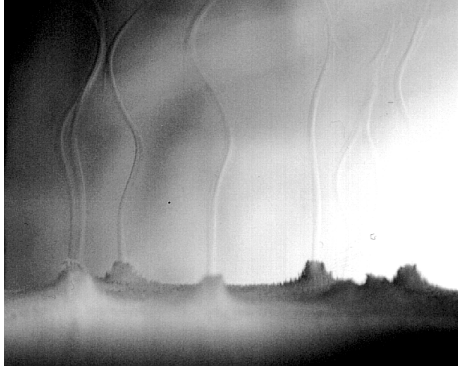


Fig. 6. Shadowgraph picture of organized plumes above an advancing solidification front.

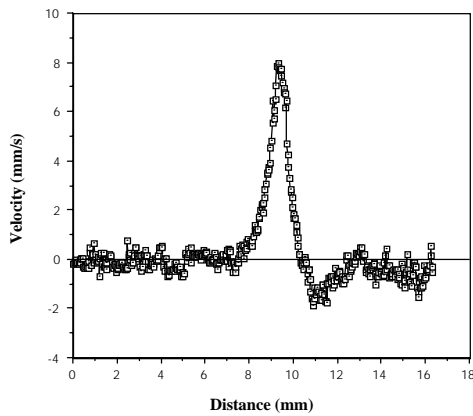


Fig. 7. Velocity profile across a plume measured by MTV line tagging.

formed from a large number of fine structures later in the solidification process⁴⁶.

Measurement of this flow field by particle-based techniques is problematic since the presence of particles could interfere with the solidification process and create unwanted nucleation sites. The MTV approach using phosphorescent supramolecules was used to measure the velocity profile across a plume for the first time⁴⁶. A line was tagged across the plume and its displacement was interrogated 60 ms later. Such a long delay was required due to the slow flow speeds involved. Figure 7 shows the measured instantaneous velocity profile across a single plume. The upward jet-like velocity field within the plume is captured along with a non-symmetric downward flow around the plume. Note the peak velocity is only 8 mm/s (nearly 8 pixel displacement) and the width of the plume is about 2 mm. Also of interest is the fact that the delay time for interrogation is 12 times longer than the phosphorescence lifetime (i.e. e^{-1} point) of the tracer, requiring the use of an intensified camera for detection.

4.3 Measurements in a “Steady Flow Rig” Model of an IC Engine

This example illustrates a gas-phase application of MTV based on the phosphorescence of biacetyl. The steady flow rig configuration is commonly used in the IC engine research community to study the fundamentals of the intake flow.

The rig consists of a quartz cylinder of radius $R_0 = 41$ mm, placed axisymmetrically around a nozzle with a valve body placed axisymmetrically inside the jet nozzle. In this case the flow exiting through the valve opening, which simulates the intake flow into an IC engine geometry, is in the form of an annular jet. In this study, the valve opening (valve lift) is set at $\ell = 9$ mm and the maximum intake speed is about 10 m/s. The instantaneous accelerations in the shear layer at the interface between the intake jet and adjacent fluid can be as high as 5000 g, making it difficult to rely on the results of particle-based techniques. The details of this work can be found elsewhere^{41,42}.

Figure 8 displays a 3 cm \times 3 cm field of view in the nitrogen/biacetyl flow being investigated and the regions tagged by a grid pattern. Part of the valve body and the left wall of the cylinder are visible in the picture. The maximum flow speed in the annular jet entering the cylinder is about 10 m/s. Also shown is an example of the later image of the tagged regions after a 50 μ s delay. For this time delay, the maximum displacement of tagged regions is about 8 pixels (≈ 500 μ m). Image pairs such as those in Figure 8 have been used to determine the instantaneous radial and axial velocity components in this flow field. An example of the instantaneous velocity field and the structure of the intake flow in this geometry is shown in Figure 9 along with the average velocity field based on 320 realizations. The instantaneous flow map shows a highly unsteady intake annular jet, which has an undulating appearance with opposite sign large scale vortical structures on its two sides. The mean flow map indicates a large scale region of recirculation in the upper left corner of the engine cylinder, a feature typical of an IC engine flow field. These data have also been used to derive other properties of the flow such as the instantaneous and average vorticity fields and velocity fluctuations^{41,42}.

4.4 Velocity Field during Late Compression in IC Engine

This study highlights the utility of MTV diagnostics in a highly unsteady flow at a relatively high temperature. Using nitrogen seeded with biacetyl as the working fluid, velocity field data were obtained using MTV during late compression of an internal combustion

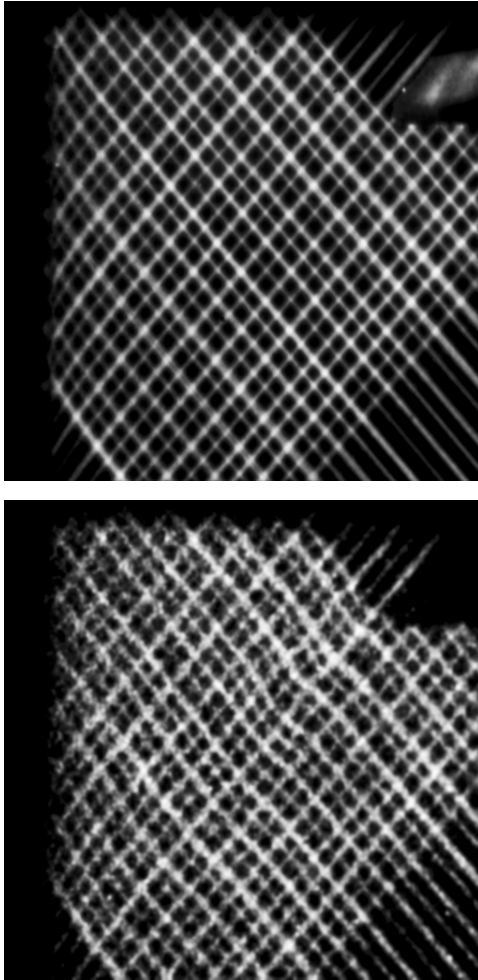


Fig. 8. Example of the tagging pattern: right after laser firing (top), and 50 μ s later (bottom).

engine, the most critical time of the four-stroke cycle. Such data are highly sought since the state of the flow just before the firing of the spark plug directly influences the subsequent combustion and emission production. A motored research engine operating at a compression ratio of 10 was utilized. Figure 10 depicts four independent samples of the velocity map at a crank angle CA = 296 degrees, as the piston approaches the Top Dead Center (TDC) of the engine. At the late compression condition described here the gas temperature can reach a value as high as 600K. In the configuration studied, it is found that the cycle-to-cycle variability can cause high velocity fluctuations exceeding 50% of the mean value⁴⁷. The velocity vector density in Figure 10 is much lower than previous examples shown; the primary goal here was to establish the feasibility of such measurement at these temperatures. This work is continuing with the purpose of quantifying and understanding the cycle-to-cycle variability in an internal combustion engine.

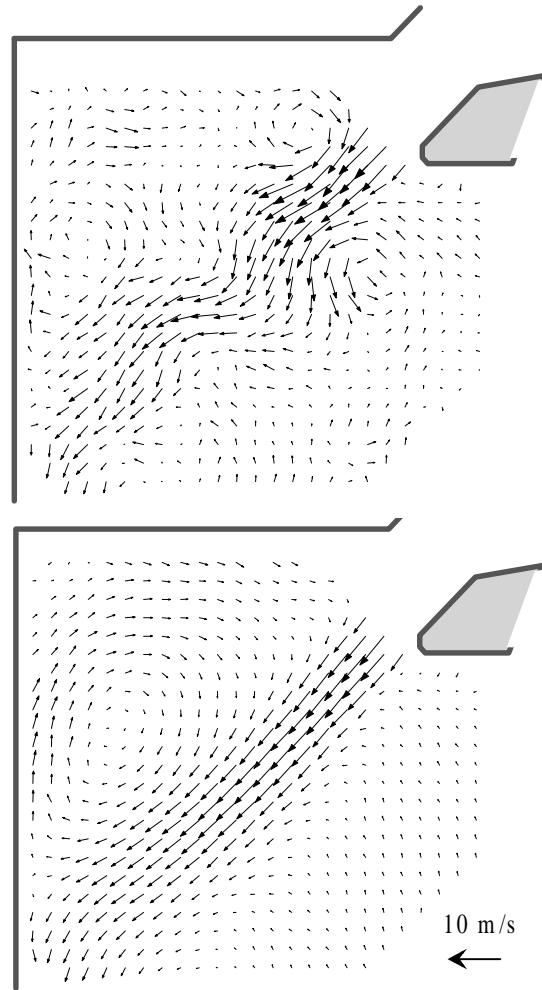


Fig. 9. Instantaneous (top) and average (bottom) velocity field in the steady flow rig model of an IC engine.

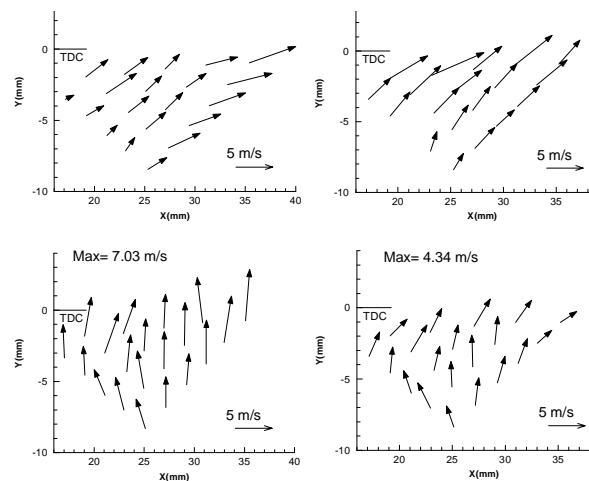


Fig. 10. Four instantaneous velocity maps using MTV at a crank angle CA = 296 degrees in an IC engine.

4.5 Simultaneous Flow Visualization/Passive Scalar and Velocity Measurements

One advantage of molecular tagging velocimetry is that it may be combined with other molecular techniques, such as laser induced fluorescence (LIF), to allow the simultaneous measurements of multiple variables in a flow. An example is given here to demonstrate the utility of this approach; other approaches and examples have been given previously^{2,18}.

In fluid flow studies it is common to visualize the overall structure of the flow using a passive scalar marker to label the flowing stream. However, it is the structure and dynamics of the vorticity field which determine the flow behavior. By combining standard LIF techniques using fluorescein and MTV using the phosphorescent supramolecules, we have developed a

means to simultaneously measure the vorticity field and visualize the structure generated by this field⁴⁸⁻⁵⁰. This is done by taking advantage of the minimal interaction between the two molecules due to their spectral characteristics. The examples shown in Figure 11 illustrate the connection between the vorticity field and the resulting flow structure in a perturbed two-stream wake. The grid tagging pattern used for MTV is also utilized for LIF and allows the visualization of the lower stream seeded with fluorescein. A CCD camera acquires the LIF image during the 20ns pulse of the laser, while a 2-detector arrangement records the MTV image pairs generated from the same laser pulse. Results in Figure 11 show that for a high perturbation amplitude the vorticity contours are centered about the cores of the "jelly-roll" patterns shown by the flow visualization. At low perturbation amplitude, however, the vorticity contours reveal regions of vorticity that are not readily identified by flow visualization alone. Since the LIF images can be quantified to yield passive scalar mixing data, the approach just described can be used to obtain simultaneous measurements of the velocity and passive scalar concentration fields. This has been done in a turbulent mixing layer, leading to the measurement of the profiles of velocity-concentration correlations⁴⁸⁻⁵⁰.

4.6 Three-Component Velocimetry

The final example presented here gives preliminary results from ongoing work to extend the MTV technique to measure all three components of the velocity vector over a plane. The approach uses stereo imaging in much the same manner as that implemented in machine vision and stereo PIV. This new capability is demonstrated in mapping the highly three-dimensional flow field near a model boat propeller rotating at 250 rpm inside a closed

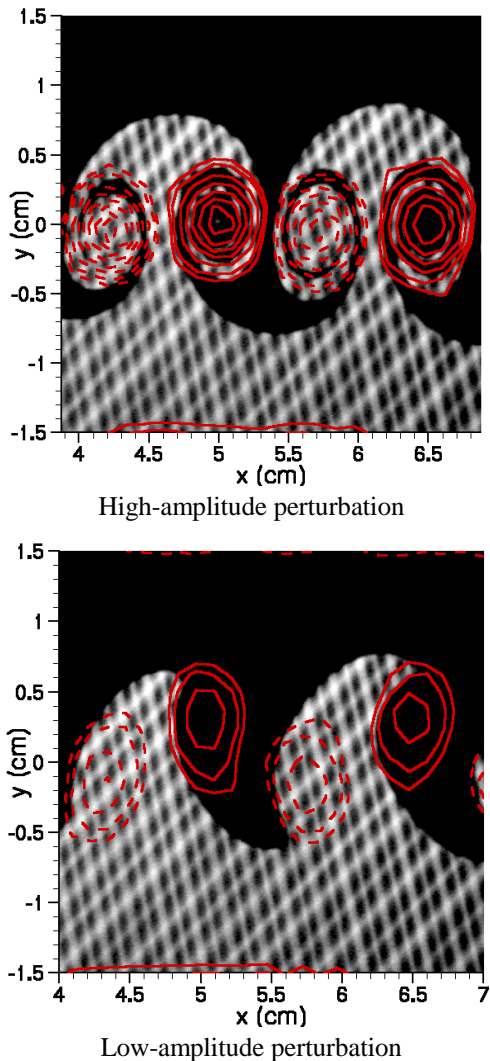


Fig. 11. Simultaneous flow visualization and vorticity field in a forced wake.

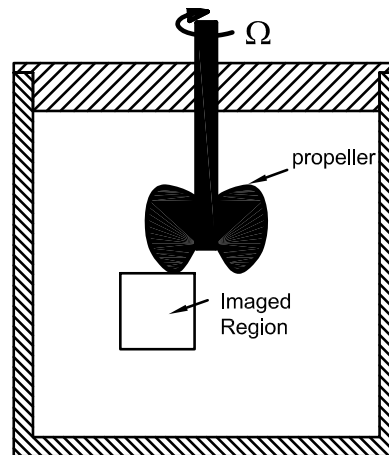


Fig. 12. Schematic of the model boat propeller and the region imaged for 3-component MTV measurements.

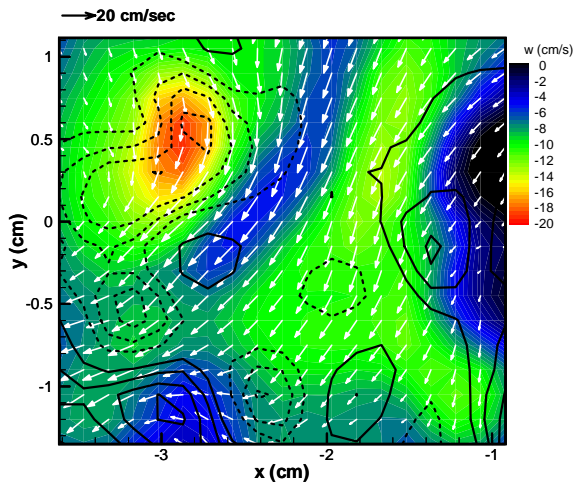


Fig. 13. Instantaneous 3-component velocity field and spanwise vorticity under a model propeller. Out of plane velocity is indicated by flooded contours. Vorticity is indicated by line contours with levels $\pm 10, \pm 20, \dots$ (s^{-1}). Dashed lines denote negative vorticity.

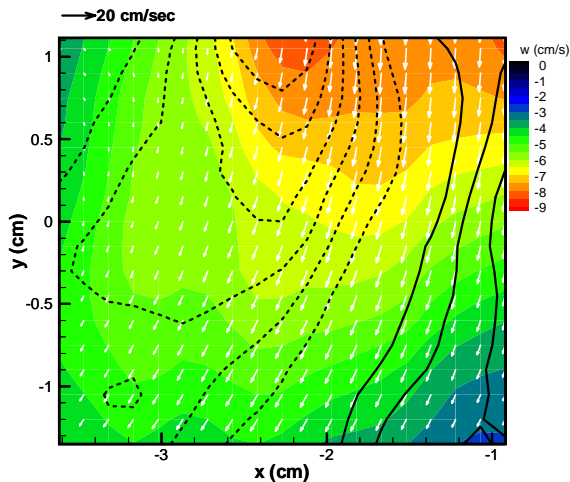


Fig. 14. Mean 3-component velocity field and spanwise vorticity under a model propeller. Out of plane velocity is indicated by flooded contours. Vorticity is indicated by line contours with levels $\pm 2, \pm 4, \dots$ (s^{-1}). Dashed lines denote negative vorticity.

container, see Figure 12. The imaged region is approximately $3 \text{ cm} \times 3 \text{ cm}$. An example of the instantaneous measurement of the three components (u, v, w) of the velocity field and the spanwise vorticity field (ω_z) is provided in Figure 13, and the corresponding mean field is depicted in Figure 14. The instantaneous field indicates a strong out of plane motion with all three components of the velocity field nearly equal. It is interesting to note that the highest level of

out of plane velocity (i.e. w) occurs in a well defined peak nearly at the same location as the (negative) peak of spanwise vorticity. The mean field clearly shows the predominant downward flow generated by the propeller.

5. Conclusions

Recent progress in Molecular Tagging Velocimetry and its applications in gas-phase and liquid-phase flows have been described. This measurement technique can be thought of as the *molecular* counterpart of PIV, and complements it where the use of seed particles is either not desirable or may lead to complications. Molecular tagging velocimetry can also be combined with other molecular techniques, such as laser induced fluorescence (LIF), to allow the simultaneous measurements of multiple variables in a flow. This method of velocimetry has continuously evolved and is now being utilized as a useful tool for fluid flow studies. As new molecular tracers become available, the variety of flow environments to which this method of velocimetry may be applied is expected to expand. Using phosphorescent tracers, application of MTV to several flow fields are described to highlight some of the capabilities of this technique. The examples include boundary-layer resolved measurements of unsteady boundary layer separation, slow convective flow in directional solidification, intake flow into a model IC engine, the hot flow in late compression of a motored IC engine, and three-component velocimetry using stereo imaging.

Acknowledgments

The MTV developments at MSU are a joint collaboration with Drs. Daniel Nocera and Harold Schock. These developments are the result of the hard work of many of my past and present graduate students and research associates: Drs. Charles Gendrich, Richard Cohn, Colin MacKinnon, Bernd Stier, and Messrs. Gregory Ambrose, Douglas Bohl, and Hooman Rezaei. This work was supported by the MRSEC Program of the National Science Foundation, Award Numbers DMR-9400417 and DMR-9809688, along with partial support by the Air Force Office of Scientific Research under grants F49620-92-J-0338 and F49620-95-1-0391.

6. References

1. Falco, R. E. and Nocera, D. G. [1993] Quantitative multipoint measurements and visualization of dense solid-liquid flows using laser induced photochemical anemometry (LIPA), in *Particulate Two-Phase Flow*, Ed. M. C. Rocco; Butterworth-Heinemann, 59-126.
2. Koochesfahani, M. M., Cohn, R. K., Gendrich, C. P., and Nocera, D. G. [1996] Molecular tagging diagnostics for

the study of kinematics and mixing in liquid phase flows, *Proceedings of the Eighth International Symposium on Applications of Laser Techniques to Fluid Mechanics*. Lisbon, Portugal, July 8-11: 1.2.1-1.2.12.

3. Popovich, A. T. and Hummel, R. L. [1967] A new method for non-disturbing turbulent flow measurement very close to a wall, *Chem. Eng. Soc.*, vol. 22, 21-25.

4. Ojha, M., Cobbold, R. S. C., Johnston, K. W., and Hummel, R. [1989] Pulsatile flow through constricted tubes: an experimental investigation using photochromic tracer methods, *J. Fluid Mech.*, vol. 203, 173-197.

5. Falco, R. E. and Chu, C. C. [1987] Measurement of two-dimensional fluid dynamic quantities using a photochromic grid tracing technique, *SPIE*, vol. 814, 706-710.

6. Douglas, P., Enos, R. D., Azzopardi, B., and Hope, C. B. [1991] Characterisation of a photochromic triarylmethane dye sulphite and its applications to the visualisation of water flows, *7th Int. Topical Meeting on Photoacoustic and Photothermal Phenomena*, The Netherlands, August, 1991.

7. Yurechko, V. N. and Ryazantsev, Yu. S. [1991] Fluid motion investigation by the photochromic flow visualization technique, *Exp. Thermal and Fluid Sci.*, vol. 4, 273-288.

8. Chu, C. C. and Liao, Y. Y. [1992] A quantitative study of the flow around an impulsively started circular cylinder, *Exp. Fluids*, vol. 13, 137-146.

9. Chu, C. C., Wang, C. T., and Hsieh, C. H. [1993] An experimental investigation of vortex motions near surfaces, *Phys. Fluids A*, vol. 5, no. 3, 662-676.

10. Couch, G. G., Johnston, K. W., and Ohja, M. [1996] Full-field flow visualization and velocity measurement with a photochromic grid method, *Meas. Sci. Technol.*, vol. 7, no. 9, 1238-1246.

11. Lempert, W. R., Magee, K., Ronney, P., Gee, K. R., and Haughland, R. P. [1995] Flow tagging velocimetry in incompressible flow using photo-activated nonintrusive tracking of molecular motion (PHANTOMM), *Exp. Fluids*, vol. 18, 249-257.

12. Harris, S. R., Lempert, W. R., Hersh, L., Burcham, C. L., Saville, A., Miles, R. B., Gee, K., and Haughland, R. P. [1996] Quantitative measurements on internal circulation in droplets using flow tagging velocimetry, *AIAA J.*, vol. 34, no. 3, 449-454.

13. Biage, M., Harris, S. R., Lempert, W. R., and Smits, A. J. [1996] Quantitative velocity measurements in turbulent Taylor-Couette flow by PHANTOMM flow tagging, *Proceedings of the Eighth International Symposium on Applications of Laser Techniques to Fluid Mechanics*, Lisbon, Portugal, July 8-11, 1996, 15.4.1-15.4.8.

14. Harris, S. R., Miles, R. B., and Lempert, W. R. [1996] Observations of fluid flow produced in a closed cylinder by a rotating lid using the PHANTOMM (Photo-Activated Non Intrusive Tracking of Molecular Motion) flow tagging technique, *Proceedings of the Eighth International Symposium on Applications of Laser Techniques to Fluid Mechanics*, Lisbon, Portugal, July 8-11, 1996, 15.3.1-15.3.9.

15. Ponce, A., Wong, P. A., Way, J. J. and Nocera, D.

G. [1993] Intense phosphorescence triggered by alcohols upon formation of a cyclodextrin ternary complex, *J. Physical Chem.*, vol. 97, 11137-11142.

16. Hartmann, W. K., Gray, M. H. B., Ponce, A., and Nocera, D. G. [1996] Substrate induced phosphorescence from cyclodextrin · lumophore host-guest complexes, *Inorg. Chim. Acta*, vol. 243, 239.

17. Mortellaro, M. A. and Nocera, D. G. [1996] A turn-on for optical sensing, *Chemtech*, vol. 26, 17-23.

18. Gendrich, C.P., Koochesfahani, M.M., and Nocera, D.G. [1997] Molecular tagging velocimetry and other novel applications of a new phosphorescent supramolecule, *Exp. Fluids*, vol.22, 67-77.

19. Stier, B. [1994] An investigation of fluid flow during the induction stroke of a water analog model of an IC engine using an innovative optical velocimetry concept -- LIPA, PhD thesis, Michigan State University.

20. Hill, R. B. and Klewicki, J. C. [1994] Developments and Applications of laser induced photochemical anemometry. *ASME Fluid Egr Div* 191, Laser Anemometry - 1994: Advances and Applications, 209-216.

21. Hill, R. B. and Klewicki, J. C. [1996] Data reduction methods for flow tagging velocity measurements, *Exp. Fluids*, vol. 20, no. 3, 142-152.

22. Gendrich, C. P., Bohl, D., and Koochesfahani, M. M. [1997] Whole field measurements of unsteady separation in a vortex ring/wall interaction, AIAA Paper No. AIAA-97-1780.

23. Gendrich, C. P. [1999] Dynamic stall of rapidly pitching airfoils: MTV experiments and Navier-Stokes simulations, PhD thesis, Michigan State University.

24. Cohn, R. K. [1999] Effect of forcing on the vorticity field in a confined wake, PhD thesis, Michigan State University.

25. Miles, R., Cohen, C., Connors, J., Howard, P., Huang, S., Markovitz, E., and Russell, G. [1987] Velocity measurements by vibrational tagging and fluorescent probing of oxygen, *Optics Letters*, vol. 12, no. 11, 861-863.

26. Miles, R. B., Connors, J. J., Markovitz, E. C., Howard, P. J., and Roth, G. J. [1989] Instantaneous profiles and turbulence statistics of supersonic free shear layers by Raman Excitation plus Laser-Induced Electronic Fluorescence (RELIEF) velocity tagging of oxygen, *Exp. Fluids*, vol. 8, 17-24.

27. Miles, R. B., Zhou, D., Zhang, B., Lempert, W. R., and She, Z. S. [1993] Fundamental turbulence measurements by RELIEF flow tagging, *AIAA J.*, vol. 31, no. 3, 447-452.

28. Miles, R. B. and Lempert, W. R. [1997] Quantitative flow visualization in unseeded flows, *Ann. Rev. Fluid Mech.*, vol. 29, 285-326.

29. Pitz, R. W., Brown, T. M., Nandula, S. P., Skaggs, P. A., DeBarber, P. A., Brown, M. S., and Segall, J. [1996] Unseeded velocity measurement by ozone tagging velocimetry, *Optics Letters*, vol. 21, no. 10, 755-757.

30. Pitz, R. W., Ribarov, L. A., Wehrmeyer, J. A., Batliwala, F., and DeBarber, P. A. [1998] Ozone tagging

velocimetry for unseeded velocity measurements in air flows, AIAA Paper No. AIAA-98-2610.

31. Ribarov, L. A., Wehrmeyer, J. A., Batliwala, F., Pitz, R. W., and DeBarber, P. A. [1999] Ozone tagging velocimetry using narrowband excimer lasers, *AIAA J.*, vol. 37, no. 6, 708-714.

32. Boedecker, L. R. [1989] Velocity measurements by H₂O photolysis and laser-induced fluorescence of OH, *Optics Letters*, vol. 14, no. 10, 473-475.

33. Goss, L., Chen, T., Trump, D., Sarka, B., and Nejad, A. [1991] Flow tagging velocimetry using UV-photodissociation of water vapor, AIAA Paper No. AIAA-91-0355.

34. Wehrmeyer, J. A., Ribarov, L. A., Oguss, D. A., Batliwala, F., Pitz, R. W., and DeBarber, P. A. [1999] Flow tagging velocimetry for low and high temperature flowfields, AIAA Paper No. AIAA-99-0646.

35. Wehrmeyer, J. A., Ribarov, L. A., Oguss, D. A., and Pitz, R. W. [1999] Flame flow tagging velocimetry with 193 nm H₂O photodissociation, submitted to *Applied Optics*.

36. Hiller, B., Booman, R.A., Hassa, C., and Hanson, R.K. [1984] Velocity visualization in gas flows using laser-induced phosphorescence of biacetyl, *Rev. Sci. Inst.*, vol. 55, 1964-1967.

37. Liu, J.B., Pan, Q., Liu, C.S. and Shi, J.R. [1988] Principles of flow field diagnostics by laser induced biacetyl phosphorescence, *Exp. in Fluids*, vol. 6, 505-513.

38. Lowry, H.S. [1987] Velocity measurements using the laser-induced phosphorescence of biacetyl, AIAA Paper No. 87-1529.

39. Hilbert, H. S. and Falco, R. E. [1991] Measurements of flows during scavenging in a two-stroke engine, SAE Technical Paper 910671.

40. Stier, B. and Koochesfahani, M.M. [1997] Molecular tagging velocimetry in gas phase and its application to jet flows, *Proceedings of ASME Fluids Engng Division Summer Meeting*, Paper FEDSM97-3687, Vancouver, June 22 - 26, 1997.

41. Stier, B. and Koochesfahani, M. M. [1998] Whole field MTV measurements in a steady flow rig model on an IC engine, SAE Technical Paper #980481.

42. Stier, B. and Koochesfahani, M. M. [1999] Molecular tagging velocimetry (MTV) measurements in gas phase flows, *Exp. in Fluids*, vol. 26, no. 4, 297-304.

43. Lu, L. J. and Smith, C. R. [1985] Image processing of hydrogen bubble visualization for determination of turbulence statistics and bursting characteristics, *Exp. Fluids*, vol. 3, 349-356.

44. D'Arco, A., Charmet, J. C., and Cloitre, M. [1982] Nouvelle technique de marquage d'écoulement par utilisation de molécules photochromes, *Revue Phys. Appl.*, vol. 17, 89-93.

45. Gendrich, C. P. and Koochesfahani, M. M. [1996] A spatial correlation technique for estimating velocity fields using Molecular Tagging Velocimetry (MTV), *Exp. Fluids*, vol. 22, no. 1, 67-77.

46. Wirtz, K., Koochesfahani, M. M., McGrath, J. J.,

and Benard, A. [1998] Molecular tagging velocimetry applied to buoyancy-driven convective phenomena during solidification, ASME Paper HTD-Vol. 361-4, 103.

47. Hascher, H. G., Novak, M., Lee, K., Schock, H., Rezaei, H., and Koochesfahani, M. M. [1998] An evaluation of IC-engine flow with the use of modern in-cylinder measuring techniques, AIAA Paper No. AIAA-98-3455.

48. MacKinnon, C. G. [1998] Effects of 2-D and 3-D forcing on molecular mixing in a two-stream shear layer, PhD thesis, Michigan State University.

49. Koochesfahani, M. M. and MacKinnon, C. G. [1998] Methods for simultaneous velocity/passive scalar measurements using molecular tagging diagnostics, presented at the 13th U.S. National Congress of Applied Mechanics, June 21-26, 1998, Gainesville, Florida.

50. Koochesfahani, M. M. and MacKinnon, C. G. [1998] Simultaneous velocity/passive scalar measurements using a molecular tagging technique, *Bull. Am. Phys. Soc.*, vol.43, no.9, 1989.